Analysis of Whole-Body Branched-Chain Amino Acid Metabolism in Mice Utilizing 20% Leucine $^{13}C_6$ and 20% Valine $^{13}C_5$ Mouse Feed

Jared R. Mayers, Margaret E. Torrence, Brian P. Fiske, Shawn M. Davidson, and Matthew G. Vander Heiden
Koch Institute for Integrative Cancer Research and Department of Biology
Massachusetts Institute of Technology, Cambridge, MA USA

Cancer cells have altered metabolism relative to normal cells. To date, most cancer metabolism research has focused on understanding the mechanisms of cell autonomous metabolic alterations such as the influence of different oncogenic signals on nutrient utilization and the effects of altered regulation of specific enzymes on metabolic fluxes through different pathways (Cairns, et al., 2011). While these studies have provided insight into metabolic needs of proliferating cancer cells (Vander Heiden, et al., 2009), they do not address potential interactions between tumor and normal tissues.

Research on whole-body metabolic alterations associated with type 2 diabetes (T2DM) provides insight into how altered metabolite sensing can affect the metabolism of specific tissues. Intriguingly, there are clear epidemiological connections between diabetes and several types of cancer, especially pancreatic adenocarcinoma (PDAC) (Everhart and Wright, 1995; Wang, et al., 2003). Indeed, epidemiologic evidence indicates that pancreatic cancer can be both a consequence of longstanding diabetes (Ben, et al., 2011) and cause of new-onset cases (Huxley, et al., 2005). Methods to study metabolism across tissues are needed to understand how whole-body metabolic alterations influence tumor metabolism, and to understand the systemic changes associated with metabolic disease.

In a recent study, we found that elevated branched-chain amino acids (BCAAs – leucine, isoleucine and valine) are found in the serum of patients with early pancreatic cancers (Mayers, et al., 2014). Using a genetically engineered mouse model of PDAC (Bardeesy, et al., 2006) we used isotope-labeled diets to assess the sources of these plasma BCAA elevations and distinguish between short-term pools defined by acute dietary uptake and disposal, and long-term pools defined by turnover of whole-body protein stores.

In this note, we describe the experimental approaches we used to define the contribution of each of these pools to plasma BCAA levels. A critical tool for these experiments was the custom-designed 20% leucine $^{13}C_6$ and 20% valine $^{13}C_5$ mouse feed diet developed in collaboration with Cambridge Isotope Laboratories, Inc. (CIL) and Harlan Laboratories, Inc.

Experimental Design

Experimental mice. Four-week-old male mice on a mixed background were used in the studies described in this note.

^{13}C-BCAA amino acid-defined diet. 20% $^{13}C_6$-Leu and 20% $^{13}C_5$-Val-labeled diets were based on diet TD.110839 and produced by CIL and Harlan.

Acute uptake and disposal. Following a 16-hour overnight fast, mice were fed the ^{13}C-BCAA diet for two hours before removal of food. Food consumption during this period was measured. At the time points indicated by the orange bars in Figure 1a, approximately 20 μL of plasma was harvested from the tail vein of conscious mice in a heparinized tube and centrifuged to separate plasma. Plasma was subsequently analyzed via gas chromatography/mass spectrometry (GC/MS) to determine the number of ion counts of ^{13}C-labeled species. This number was normalized to food intake over the two-hour feeding window for each animal.

Long-term contributions to BCAA plasma pools. Mice were fed ^{13}C-BCAA diets from seven days of age to 24 days of age followed by three days of unlabeled diet per the experimental outline in Figure 2a. Two cohorts of mice were used in this experiment. One cohort of mice was sacrificed on day 27 (fed state) and a second cohort of mice was sacrificed on day 28 after a 16-hour overnight fast (the points indicated by the orange bars in Figure 2a). Mice
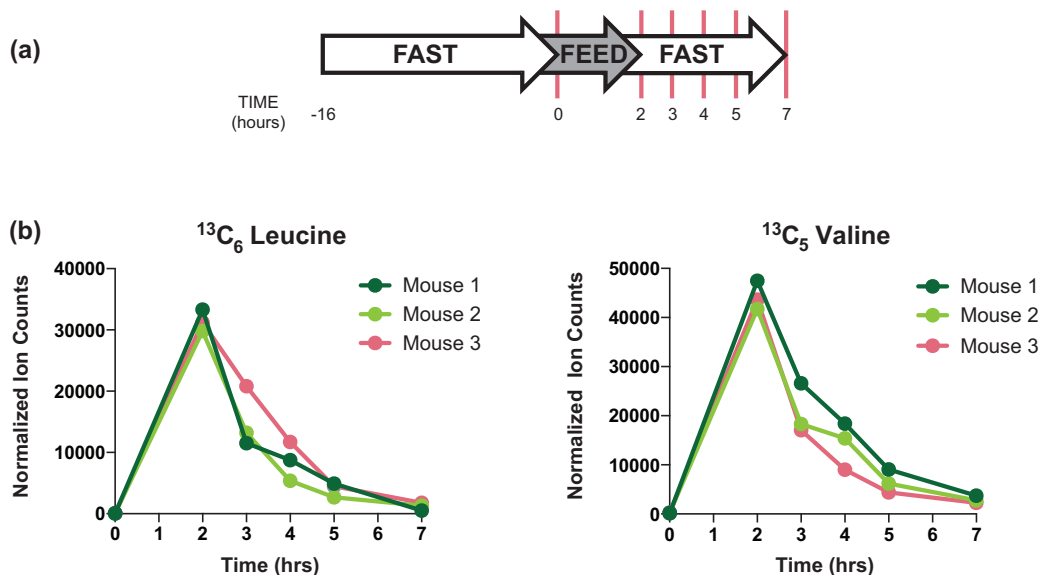
Figure 1. Assessing the kinetics of BCAA uptake and disposal. (a) Protocol for administering ^{13}C-BCAA diet and sampling blood to assess short-term pool contributions to plasma BCAA levels. (b) Normalized ion counts of ^{13}C-BCAAs in plasma.

were terminally bled and tissues harvested within five minutes, and snap frozen in liquid nitrogen using Biosqueezer (BioSpec Products). Both plasma and tissues were stored at -80°C for subsequent GC/MS analysis.

Based on fractional labeling patterns of leucine and valine, we calculated the total contributions from short- and long-term pools according to the following equations:

$$Long\text{-}Term\ Pool = \left(\frac{Fed\ \%\ Labeled}{Fasted\ \%\ Labeled}\right) \times Relative\ Fed\ Pool\ Size$$

$$Short\text{-}Term\ Pool = Relative\ Fed\ Pool\ Size - Long\text{-}Term\ Pool$$

GC/MS analysis. Plasma polar metabolites were extracted in ice-cold 4:1 methanol:water with norvaline internal standard (5 µL plasma in 200 µL extraction solution). Extracts were clarified by centrifugation and the supernatant evaporated under nitrogen and frozen at -80°C for subsequent derivitization. Dried polar metabolites were dissolved in 20 µL of 2% methoxyamine hydrochloride in pyridine (Thermo) and held at 37°C for 1.5 hours. After dissolution and reaction, *tert*-butyldimethylsilyl derivatization was initiated by adding 25 µL *N*-methyl-*N*-(*tert*–butyldimethylsilyl) trifluoroacetamide + 1% *tert*-butyldimethylchlorosilane (Sigma) and incubating at 37°C for one hour. The acid hydrolysis protocol was adapted from Antoniewicz and colleagues (Antoniewicz, et al., 2007). Briefly, acid hydrolysis of tissue proteins was performed on snap frozen tissues by boiling 1-5 mg tissue in 1 mL 18% hydrochloric acid overnight at 100°C. 50 µL supernatant was evaporated under nitrogen and frozen at -80°C for subsequent derivitization. Dried hydrolysates were redissolved in pyridine (10 µL/1 mg tissue) prior to *tert*-butyldimethylsilyl derivatization, which was initiated by adding *N*-methyl-*N*-(*tert*-butyldimethylsilyl) trifluoroacetamide +1% *tert*-butyldimethylchlorosilane (12.5 µL/ 1 mg tissue, Sigma) and incubating at 37°C for one hour.

GC/MS analysis was performed using an Agilent 7890 GC equipped with a 30m DB-35MS capillary column connected to an Agilent 5975B MS operating under electron impact ionization at 70 eV. One µL of sample was injected in splitless mode at 270°C, using helium as the carrier gas at a flow rate of 1 mL min^{-1}. For measurement of amino acids, the GC oven temperature was held at 100°C for three minutes and increased to 300°C at 3.5°C min^{-1}. The MS source and quadrupole were held at 230°C and 150°C, respectively, and the detector was run in scanning mode, recording ion abundance in the range of 100-605 *m/z*. MIDs were determined by integrating the appropriate ion fragments (Antoniewicz, et al., 2007) and corrected for natural isotope abundance using an algorithm adapted from Fernandez and colleagues (Fernandez, et al., 1996).

Results

Assessing the kinetics of BCAA uptake and disposal. Utilizing the experimental approach outline in Figure 1a, we fasted mice overnight before drawing a baseline blood sample and feeding mice the ^{13}C-BCAA containing diet for two hours. As the liver does not regulate plasma BCAA levels (Brosnan, 2003; Matthews, et al., 1993) all ^{13}C-BCAAs absorbed from the gut will enter the bloodstream for subsequent disposal via catabolism or protein incorporation in peripheral tissues (Harper, et al., 1984).

Sampling of blood immediately at the conclusion of the two-hour feed showed consistent gut absorption across animals when normalized to food intake (Figure 1b). Food was subsequently removed and animals serially bled to track the rate of disappearance of ^{13}C-BCAAs from blood. The disposal curves were similar across animals and revealed a rapid rate of disposal with virtually all ^{13}C-BCAAs removed from the bloodstream within five hours after feeding (Figure 1b).
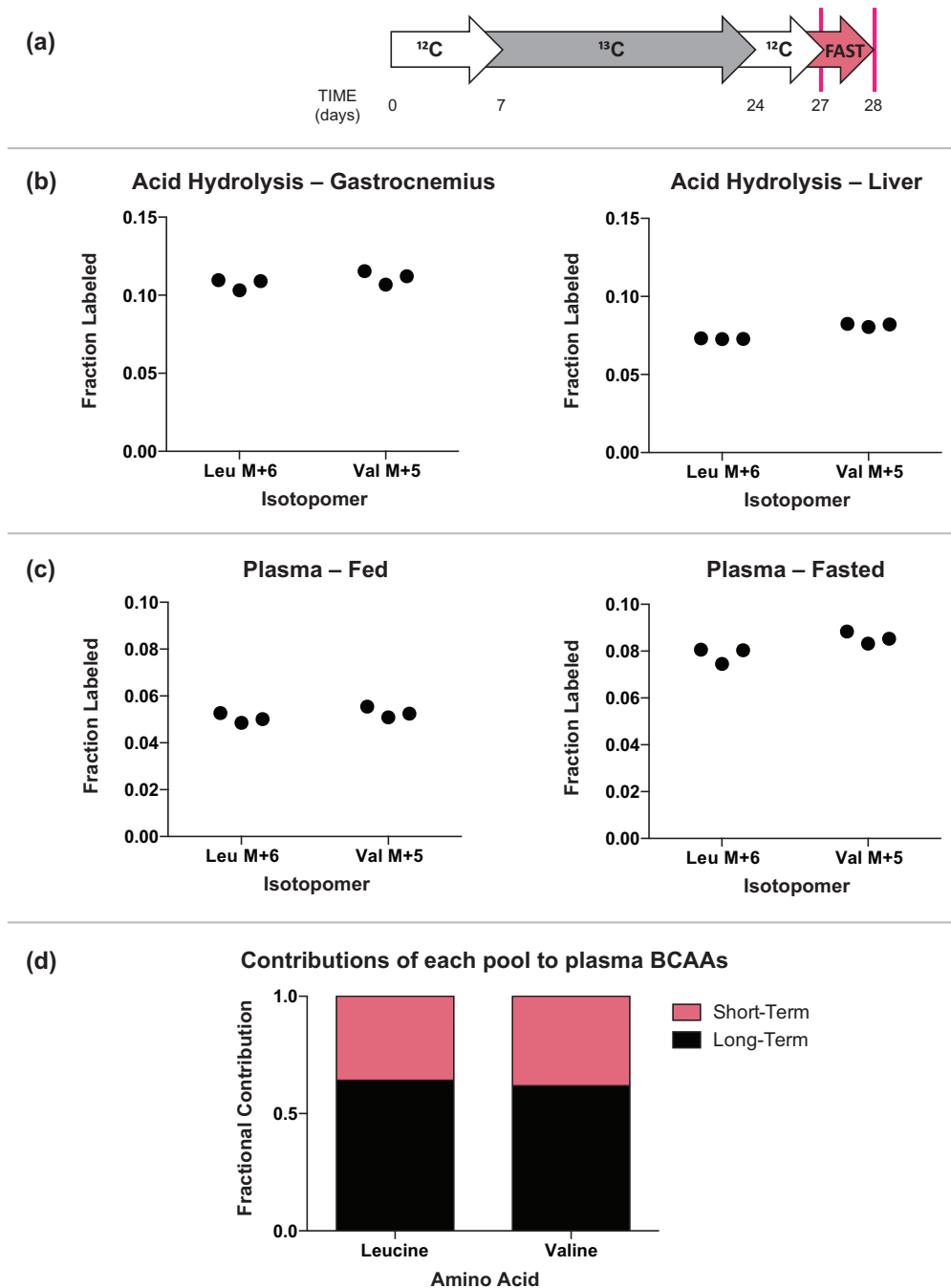
Figure 2. Assessing turnover of long-term protein stores. (a) Protocol for administering ¹³C-BCAA diets and sacrificing mice to determine the contribution to plasma BCAA levels from the turnover of long-term protein stores. (b) Acid hydrolysis of tissue protein demonstrating incorporation of labeled amino acids derived from ¹³C-BCAAs. (c) Fractional labeling of BCAAs in fed (left) and fasted (right) state. (d) Calculation derived from data in part (c) demonstrating relative contributions of the short- and long-term pools to plasma BCAA levels.

Assessing turnover of long-term protein stores. To examine the contributions of BCAA release into the blood resulting from the turnover of long-term tissue protein stores, we devised the protocol outlined in Figure 2a. This "pulse-chase" approach ensured incorporation of ¹³C-BCAAs into tissue protein as labeling occurred during a period of rapid growth, when the mice grow from approximately 1.5 g to 15 g. After labeling mice for 17 days,

the three-day washout period with unlabeled feed removed residual label from the short-term pool.

Following this three-day period, we sacrificed one cohort of mice in the post-prandial or fed state and a second cohort of mice after an overnight fast (Figure 2a). To analyze the amino acid composition of each tissue and measure the incorporation of ¹³C-BCAAs into

tissue protein stores, we acid-hydrolyzed gastrocnemius muscle and liver from both cohorts. In Figure 2b, we demonstrate that a diet containing 20% ^{13}C-BCAA resulted in approximately 11-12% labeling of BCAAs in muscle and 7-8% labeling in liver. The difference between these two tissues likely reflects a higher baseline rate of protein synthesis and turnover in the liver.

To quantify the contributions to plasma BCAA levels from the long- and short-term pools, we compared fractional ^{13}C labeling of plasma BCAAs in both the fed state, with inputs from both pools, and the fasted state, in which only long-term pools contribute to plasma levels (Figure 2c). Following the calculations outlined in the Methods section, we determined that turnover of long-term protein stores accounts for approximately two-thirds of plasma BCAAs in the fed state, with the remainder made up of dietary inputs (Figure 2d).

Discussion

Here we describe two approaches for determining the contribution of different pools of BCAAs to plasma levels of these amino acids. Utilizing a custom-designed 20% leucine ^{13}C$_6$ and 20% valine ^{13}C$_5$ mouse feed diet, we specifically labeled short- or long-term sources of plasma BCAAs in mice. These approaches also relied on the unique status of BCAAs as the only amino acids whose plasma levels are not regulated by the liver (Brosnan, 2003; Matthews, et al., 1993). This ensures that all ^{13}C-BCAAs consumed by the mice and absorbed from the gut are directly available to peripheral tissues for catabolism and/or incorporation into protein. Importantly, applying the methods described in this note resulted in consistent inter-mouse measurements of gut absorption, tissue disposal and whole-body protein turnover rates. Furthermore, we observe the expected concordance of labeling patterns for leucine and valine

as these amino acids share common pathways of metabolism (Harper, et al., 1984).

Altered BCAA metabolism is emerging as a consistent feature of many diseased states, such as obesity and diabetes (Newgard, et al., 2009; Wang, et al., 2011), cancer (Mayers, et al., 2014; Tonjes, et al., 2013) and starvation (Adibi, 1976). And while these changes are well described, their underlying causes remain poorly understood. Therefore, applying whole-mouse labeling approaches with the 20% leucine ^{13}C$_6$ and 20% valine ^{13}C$_5$ mouse feed will allow researchers to elucidate the precise alterations and identify the mechanisms ultimately driving these changes.

Related Products

Catalog No.	Description
MF-LEU-VAL-20	Mouse Express® L-Leucine (^{13}C$_6$, 99%) and L-Valine (^{13}C$_5$, 99%) Mouse Feed Diet contains: 20% labeled L-Leu and L-Val and 80% unlabeled L-Leu and L-Val
MLK-LYS-C	Mouse Express® L-Lysine (^{13}C$_6$, 99%) Mouse Feed Kit Kit contains: 1 kg of L-lysine (^{13}C$_6$) feed and 1 kg of (unlabeled) feed
MLK-LEU-D3	Mouse Express® L-Leucine (5,5,5-D$_3$, 98%) Mouse Feed Kit Kit contains: 1 kg of L-leucine (D$_3$) feed and 1 kg of (unlabeled) feed
MLK-SPIRULINA-N	Mouse Express® (^{15}N, 98%) Mouse Feed Kit prepared with Spirulina Kit contains: 1 kg of Spirulina (^{15}N, 98%) feed and 1 kg Spirulina (unlabeled) feed

Custom-formulated amino acid-defined diets are available in additional labeling patterns and amino acid substitutions. Please inquire.

References

Adibi, S.A. **1976**. Metabolism of branched-chain amino acids in altered nutrition. *Metab Clin Exp, 25,* 1287-1302.

Antoniewicz, M.R.; Kraynie, D.F.; Laffend, L.A.; González-Lergier, J.; Kelleher, J.K.; Stephanopoulos, G. **2007**. Metabolic flux analysis in a nonstationary system: fed-batch fermentation of a high yielding strain of *E. coli* producing 1,3-propanediol. *Metab Eng, 9,* 277-292.

Bardeesy, N.; Aguirre, A.J.; Chu, G.C.; Cheng, K.-H.; Lopez, L.V.; Hezel, A.F.; Feng, B.; Brennan, C.; Weissleder, R.; Mahmood, U.; et al. **2006**;. Both p16(Ink4a) and the p19(Arf)-p53 pathway constrain progression of pancreatic adenocarcinoma in the mouse. *Proc Natl Acad Sci USA, 103,* 5947-5952.

Ben, Q.; Xu, M.; Ning, X.; Liu, J.; Hong, S.; Huang, W.; Zhang, H.; Li, Z. **2011**. Diabetes mellitus and risk of pancreatic cancer: A meta-analysis of cohort studies. *Eur J Cancer, 47,* 1928-1937.

Brosnan, J.T. **2003**. Interorgan amino acid transport and its regulation. *J Nutr, 133,* 2068S-2072S.

Cairns, R.A.; Harris, I.S.; Mak, T.W. **2011**. Regulation of cancer cell metabolism. *Nat Rev Cancer, 11,* 85-95.

Everhart, J.; Wright, D. **1995**. Diabetes mellitus as a risk factor for pancreatic cancer. A meta-analysis. *JAMA, 273,* 1605-1609.

Fernandez, C.A.; Rosiers, Des, C.; Previs, S.F.; David, F.; Brunengraber, H. **1996**. Correction of ^{13}C mass isotopomer distributions for natural stable isotope abundance. *J Mass Spectrom, 31,* 255-262.

Harper, A.; Miller, R.; Block, K. **1984**. Branched-chain amino acid metabolism. *Annual Review of Nutrition, 4,* 409–454.

Huxley, R.; Ansary-Moghaddam, A.; Berrington de González, A.; Barzi, F.; Woodward, M. **2005**. Type-II diabetes and pancreatic cancer: a meta-analysis of 36 studies. *Br J Cancer, 92,* 2076-2083.

Matthews, D.E.; Marano, M.A.; Campbell, R.G. **1993**. Splanchnic bed utilization of leucine and phenylalanine in humans. *Am J Physiol, 264,* E109-E118.

Mayers, J.R.; Wu, C.; Clish, C.B.; Kraft, P.; Torrence, M.E.; Fiske, B.P.; Yuan, C.; Bao, Y.; Townsend, M.K.; Tworoger, S.S.; et al. **2014**. Elevation of circulating branched-chain amino acids is an early event in human pancreatic adenocarcinoma development. *Nat Med.*

Newgard, C.B.; An, J.; Bain, J.R.; Muehlbauer, M.J.; Stevens, R.D.; Lien, L.F.; Haqq, A.M.; Shah, S.H.; Arlotto, M.; Slentz, C.A. **2009**. A Branched-Chain Amino Acid-Related Metabolic Signature that Differentiates Obese and Lean Humans and Contributes to Insulin Resistance. *Cell Metab, 9,* 311-326.

Tonjes, M.; Barbus, S.; Wang, W.; Schlotter, M. **2013**. BCAT1 promotes cell proliferation via amino acid catabolism in IDH1 wildtype gliomas. *Nat Med, 1-35.*

Vander Heiden, M.G.; Cantley, L.C.; Thompson, C.B. **2009**. Understanding the Warburg effect: the metabolic requirements of cell proliferation. *Science, 324,* 1029-1033.

Wang, F.; Herrington, M.; Larsson, J.; Permert, J. **2003**. The relationship between diabetes and pancreatic cancer. *Mol Cancer, 2,* 1-5.

Wang, T.J.; Larson, M.G.; Vasan, R.S.; Cheng, S.; Rhee, E.P.; McCabe, E.; Lewis, G.D.; Fox, C.S.; Jacques, P.F.; Fernandez, C.; et al. **2011**. Metabolite profiles and the risk of developing diabetes. *Nat Med, 17,* 448-453.